Determination of the effective coercive field of ferroelectrics by piezoresponse force microscopy

M. Lilienblum and E. Soergel

Related Articles

Hysteresis mechanism in low-voltage and high mobility pentacene thin-film transistors with polyvinyl alcohol dielectric
Appl. Phys. Lett. 101, 033303 (2012)

Hysteresis mechanism in low-voltage and high mobility pentacene thin-film transistors with polyvinyl alcohol dielectric
APL: Org. Electron. Photonics 5, 152 (2012)

Evidence of temperature dependent domain wall dynamics in hard lead zirconate titanate piezoceramics
J. Appl. Phys. 112, 014113 (2012)

Thermally activated polarization dynamics under the effects of lattice mismatch strain and external stress in ferroelectric film
J. Appl. Phys. 112, 014112 (2012)

Sub-bandgap photocurrent effects on dynamic pyroelectric measurement in Pt/PbTiO3/Nb:SrTiO3 heterostructures
J. Appl. Phys. 112, 014111 (2012)
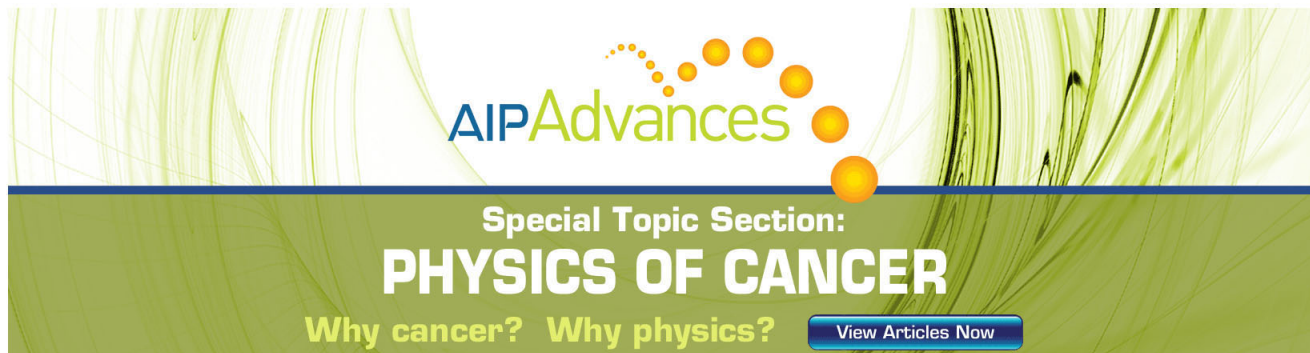
Additional information on J. Appl. Phys.

Journal Homepage: http://jap.aip.org/

Journal Information: http://jap.aip.org/about/about_the_journal

Top downloads: http://jap.aip.org/features/most_downloaded

Information for Authors: http://jap.aip.org/authors

Determination of the effective coercive field of ferroelectrics by piezoresponse force microscopy

M. Lilienblum[a)] and E. Soergel[b)]
Institute of Physics, University of Bonn, Wegelerstraße 8, 53115 Bonn, Germany

The effective coercive field E_c for ferroelectric domain reversal is usually determined in a capacitor-like geometry by increasing an applied electric field until poling occurs. Here we present a different method based on local poling with the tip of a scanning force microscope and analyzing the dependence of the domain size on the poling parameters. This method for determining E_c is of importance because for many samples the standard technique fails, either because they are too small in size, or because they are slightly conductive. Results obtained on lithium niobate crystals of different composition conform to literature values. © *2011 American Institute of Physics*. [doi:10.1063/1.3624802]

Ferroelectric materials posses a spontaneous electric polarization the direction of which can be reversed by applying an external electric field exceeding the coercive field E_c. The possibility of poling, i.e., controlled domain reversal, makes of ferroelectrics, and in particular of lithium niobate ($LiNbO_3$), a very versatile starting material, e.g., for data storage devices and nonlinear optical applications.[1] The creation of specific domain patterns is thus essential and consequently also the knowledge of E_c. In all ferroelectrics E_c is an empirical parameter significantly different from that predicted by the Ginzburg-Landau-Devonshire concept. The experimental determination of E_c is $LiNbO_3$ usually performed using a large sample sandwiched between planar electrodes, ramping up the voltage until poling starts. The starting moment can be determined by monitoring the poling current originating from the reversion of the surface polarization charging. The values obtained for E_c are known to depend on the specific experimental conditions, such as ramping speed, pre-conditioning, and electrode material. But also for nominally identical crystals from different companies E_c was found to differ substantially. Consequently the values published for E_c vary strongly (see also Table I) and rather describe an "effective coercive field," which is of more practical use than a theoretically predicted value for E_c.

Local poling with the help of the tip of a scanning force microscope (SFM) has been proven to be a powerful technique for the creation of sub-μm-sized domains.[2–4] Using domain patterns generated by this technique the highest data storage density so far could be realized.[5] But also large-area regular patterns suitable for photonic crystal applications were demonstrated.[6] Besides the aim of fabricating domain patterns for applications as described above, SFM-tip based domain formation has also been used to gain information on the sample properties, such as defect structure, wall pinning, or local switching characteristics.[7–9] In addition to the experiments, a large number of publications theoretically investigating the subject of SFM-tip based domain formation can be found.[10–12] Here in particular the modeling of the electric field distribution inside the sample, thereby taking into account the exact geometry of the probe, was investigated[13] as well as a detailed analysis of the domain nucleation process.[14] In this contribution, we demonstrate how SFM-tip based domain formation can be used to obtain a value for the effective coercive field E_c of a ferroelectric, exemplified for a series of $LiNbO_3$ crystals of different compositions.

Figure 1 shows a sketch of the three basic steps of domain formation driven by the well-localized electric field of a SFM tip. The process starts with the quasi instantaneous creation of a small domain at the sample surface ("starter domain") in a volume where the electric field E exceeds the effective coercive field E_c (Fig. 1(a)). Next the domain grows fast into the depth of the crystal in the z-direction (Fig. 1(b)). Finally the domain expands slowly by the sideways movement of the domain walls (Fig. 1(c)).

The electric field underneath the tip can be approximated by that of a point charge at distance r_{tip} from the sample surface. The normal component of the field for thin
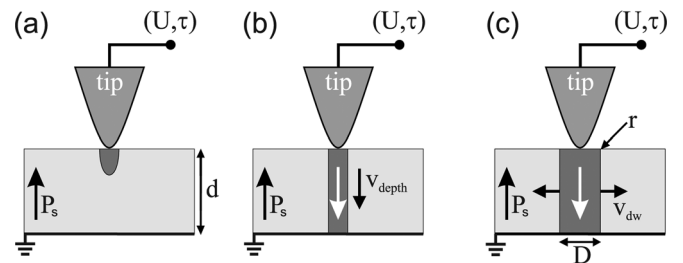

FIG. 1. Domain growth in a thin ferroelectric sample (thickness d) when a voltage pulse (amplitude U, duration τ) is applied to the tip of a SFM. (a) Instantaneous creation of a starter domain in a volume where $E \geq E_c$. (b) Fast domain propagation into the depth of the material with velocity v_{depth}, and (c) slow sideways movement of the domain walls with velocity v_{dw} resulting in a domain of width D.

a)Electronic address: lilienblum@uni-bonn.de.
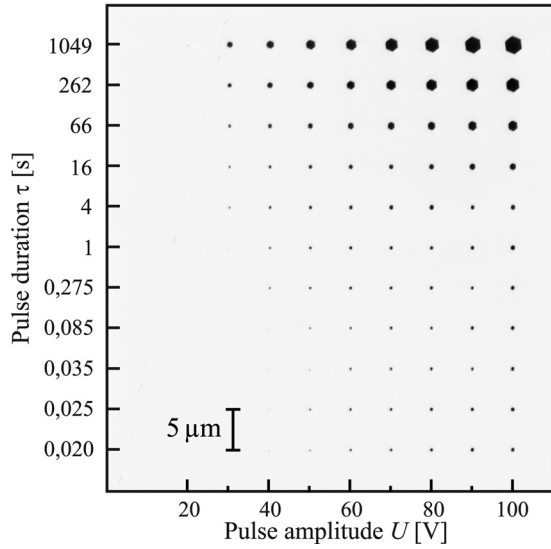b)Author to whom correspondence should be addressed. Electronic mail: soergel@uni-bonn.de.

FIG. 2. Poling map on the $+z$ face of a 13 μm thin Mg-doped nearly stoichiometric LiNbO$_3$ sample. In addition to the obvious dependence of the domain size on both the pulse duration τ and the pulse amplitude U, the hexagonal shape of the domains, typical for LiNbO$_3$, is clearly visible, in particular for the larger domains.

samples (thickness d) at the position r can then be expressed as follows:[7]

$$E = \frac{r_{tip}U}{dr} \qquad (1)$$

with U denoting the voltage applied to the tip. Using the assumption that within the area where $E \geq E_c$ a starter domain with diameter D_s is formed instantaneously, the determination of the effective coercive field E_c is straightforward, expressing r by $D_s/2$ in Eq. 1:

$$E_c = \frac{2r_{tip}U}{dD_s}. \qquad (2)$$

The effective coercive field E_c can thus be obtained by measuring the size of the starter domain D_s with the knowledge of the tip radius r_{tip}, the amplitude of the voltage pulse U, and the sample thickness d.

The velocity of the sideways movement of a domain wall v_{dw} was experimentally investigated half a century ago by R. C. Miller *et al.* in BaTiO$_3$ single crystals applying an electric field $E < E_c$ to a sample slab using large electrodes.[15,16] The sideways domain wall movement was explained with a statistical nucleation process, a model that is still in use today,[17] according the relation

$$v_{dw} = v_{\infty}e^{-(\delta/E)}, \qquad (3)$$

also known as Merz's law, where v_{∞} and the activation field δ are electric field independent parameters.[18]

As in the situation described above, sideways domain wall motion in an area where $E < E_c$ occurs also in SFM-tip based domain formation. The fact that E is inhomogeneous results only in a complex behavior of the domain growth due to the strong non-linear field dependence of Merz's law
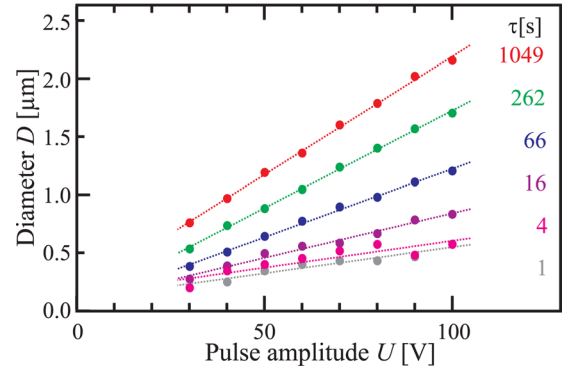

FIG. 3. (Color online) Size of the generated domains (diameter D) as a function of the pulse height U for different pulse durations τ obtained from the poling map shown in Fig. 1. The lines are linear fits to the experimental data. In order to improve clarity we only show the data for pulses $\tau \geq 1$ s.

(Eq. 3). The size D of a domain created by applying a voltage pulse (U, τ) to the SFM tip can be therefore derived as follows: From the domain wall velocity $v_{dw} = dr/d\tau$ together with Eqs. 1 and 3 we get

$$\frac{d\tau}{dr} = \frac{1}{v_{dw}} = \frac{1}{v_{\infty}}e^{(\delta/E)} = \frac{1}{v_{\infty}}e^{\alpha D}; \quad \alpha = \frac{\delta d}{2r_{tip}U}. \qquad (4)$$

Integration of Eq. 4 yields

$$\tau + c = \frac{1}{2v_{\infty}\alpha}e^{\alpha D}. \qquad (5)$$

The integration constant c, obtained by setting $\tau = 0$ and thus $D = D_s$, reads $c = 1/(2v_{\infty}\alpha)e^{\alpha D_s}$. The domain size D can now be expressed by

$$D = \frac{1}{\alpha}\ln[2v_{\infty}\alpha\tau + e^{\alpha D_s}]. \qquad (6)$$

D depends logarithmically on the pulse duration τ and in first order linearly on the applied voltage U (via $1/\alpha$), as has been observed many times (see, e.g., Refs. 2, 3, 9).

Our experiments were performed with a commercial scanning probe microscope (Solaris from NT-MDT) using conductive diamond-coated tips (DCP11 from NT-MDT). Using a custom-designed script we automatically wrote a grid of domains varying pulse amplitude U and duration τ (termed "poling map" below), for a range of U from ± 10 to ± 100 V and τ from 1 ms to 1000 s. The generated domain patterns were imaged by piezoresponse force microscopy (PFM).[19] The tip radius r_{tip} was determined before and reconfirmed after the generation of a poling map by measuring the lateral resolution when scanning across a domain boundary.[20] We carried out experiments with lithium niobate (LiNbO$_3$) crystals of various compositions, exhibiting different values of E_c. The samples were thinned down to $d = 10$ to 30 μm and glued onto an ITO-coated glass slab that was electrically grounded for the experiments.

A poling map obtained on a Mg-doped nearly stoichiometric LiNbO$_3$ (Mg:SLN) sample with $d = 13$ μm is displayed in Fig. 2. Increasing the pulse amplitude U results in larger domains the hexagonal shape of which, typical for
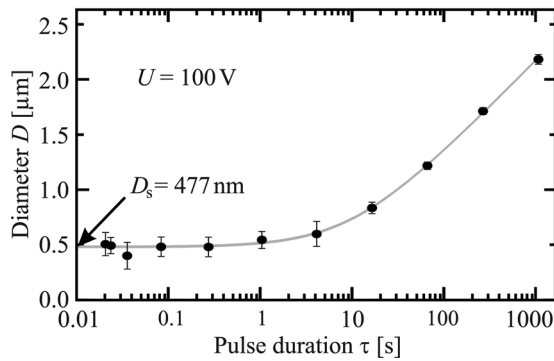
FIG. 4. Size of the generated domains (diameter D) as a function of the pulse duration τ for a fixed pulse height $U = 100$ V. The line is a fit to the experimental data using Eq. 6. The size of the starter domain D_s can be directly read from the graph.

LiNbO$_3$, is clearly seen for the larger domains. Figure 3 shows the analysis of the poling map (for clarity we only show the result for domains written with pulses $\tau \geq 1$ s). The size of every domain generated was determined and for every data set, comprising domains written by a fixed pulse duration τ and varying pulse amplitude U, a linear fit was performed. As expected from Eq. 6, for a given τ the domain size depends linearly on U. From this graph, a possible effect of crystal inhomogeneities on D can also be estimated to be only of minor importance, the scattering of the individual data points being negligible.

In Fig. 4 we plot the values of the domain diameter D versus the pulse duration τ for a fixed pulse amplitude of $U = 100$ V. We take the values obtained by the fits in Fig. 3, thereby taking the information of the whole poling map into account and thus avoiding any inaccuracies due to local crystal inhomogeneities. Obviously for pulse durations $\tau < 1$ s the size of the domains generated is constant, reflecting the characteristic of the presumed starter domain D_s. For $\tau > 10$ s the domain size D grows logarithmically with increasing pulse duration. The domains were written at different positions of the crystal, thus their sizes, and in particu-

TABLE I. Comparison of experimentally obtained and literature values for the effective coercive field E_c for different samples (SLN: stoichiometric LiNbO$_3$ and CLN: congruent LiNbO$_3$). Provenance and composition of the crystals: (1) Oxide Corp.; (2) Crystal Technology Inc.; (3) 1.3 mol. % Mg, Oxide Corp.; (4) 5 mol. % Mg, Yamaju Ceramics Co. Ltd.; (5) 3 wt. % Fe$_2$O$_3$ in the melt, Crystal Technology Inc.

Material		E_c (exp.) [kV/mm]	E_c (lit.) [kV/mm]	References
SLN (1)	$+z$	3.0	2.5–8	22, 23
	$-z$	2.9		
CLN (2)	$+z$	18.4	19–22	22, 24
	$-z$	>15		
Mg:SLN (3)	$+z$	1.7	1.8–3.9	25, 26
	$-z$	2.3		
Mg:CLN (4)	$+z$	1.4	1.3–5.0	27, 28
	$-z$	1.4		
Fe:CLN (5)	$+z$	—	—	—
	$-z$	3.3		

lar the size of D_s, is manifestly not governed by some local feature of the material; a fact that is furthermore supported by the mere size of D_s. Using now Eq. 6 to fit the experimental data displayed in Fig. 4, we can directly determine the size of the starter domain to be $D_s = 477 \pm 14$ nm. Inserting this value in Eq. 2 together with the tip radius ($r_{tip} = 72$ nm) yields $E_c = 2.32 \pm 0.07$ kV/mm for a Mg:SLN sample.

Our experimental results obtained for the different LiNbO$_3$ crystals are summarized in Table 1. The values we obtained for E_c are in general on the lower side when compared to those from the literature. We attribute this systematic behavior (i) to the simple model used and (ii) to the ambient conditions the measurements were performed in. The size of the domains generated by local poling with the SFM tip become smaller in a dry environment,[21] consequently yielding higher values for E_c (Eq. 2). The differences of E_c for the $+z$ and the $-z$ faces, respectively, reflect the error in the determination of the sample thickness. Only for magnesium-doped congruent LiNbO$_3$ (Mg:CLN) we had a two-domain sample and the poling maps for $+z$ and $-z$ were written right beside the domain boundary. In this case the values obtained for E_c match perfectly.

The measurement with CLN is strongly impeded by the high value of E_c. As a consequence, only very small domains are created, and the determination of E_c is thus deficient; on the $-z$ face we could only get a lower limit for E_c. This problem could, however, be overcome using thinner samples, and thus obtaining larger domains within the accessible amplitude of the voltage pulses. The measurement performed on the highly iron-doped crystal (Fe:CLN) illustrates the potential of our method for determining E_c. The dark conductivity of this material is too high to allow for the standard technique using large electrodes.

Finally we want to discuss the nature of the starter domain D_s. One might argue that we detect the oddments of initially larger domains that switched back partially. To rebut this assumption it is worth noting that the size of D_s is very steady; partially back switched domains, however, would not reproducibly yield domains of the same size. And also the linear dependence of the size of D_s on U, confirmed experimentally, cannot be explained by the presumption of D_s originating from oddments.

In conclusion we have succeeded in deriving values for the effective coercive field E_c in different LiNbO$_3$ single crystals from the growth behavior of SFM-tip generated domains. Our values obtained for E_c were found to be consistent with those known from the literature obtained with large samples sandwiched between planar electrodes. The determination of a value for E_c in highly iron-doped, and therefore slightly conductive, lithium niobate underlines the potential of our method. We expect this method to be applicable for any ferroelectric material and consequently to be also of interest for extremely small sized samples as they are common for explorative materials.

[1]L. Arizmendi, Phys. Status Solidi A **201**, 253 (2004).

[2]P. Paruch, T. Tybell, and J.-M. Triscone, Appl. Phys. Lett. **79**, 530 (2001).

[3]B. J. Rodriguez, R. J. Nemanich, A. Kingon, A. Gruverman, S. V. Kalinin, K. Terabe, X. Y. Liu, and K. Kitamura, Appl. Phys. Lett. **86**, 012906 (2005).

[4]M. Lilienblum, A. Ofan, Á. Hoffmann, O. Gaathon, L. Vanamurthy, S. Bakhru, H. Bakhru, R. M. Osgood, Jr., and E. Soergel, Appl. Phys. Lett. **96**, 082902 (2010).

[5]Y. Cho, S. Hashimoto, N. Odagawa, K. Tanaka, and Y. Hiranaga, Appl. Phys. Lett. **87**, 232907 (2005).

[6]A. Ofan, M. Lilienblum, O. Gaathon, A. Sehrbrock, Á. Hoffmann, S. Bakhru, H. Bakhru, S. Irsen, R. M. Osgood Jr., and E. Soergel Nanotechnology **22**, 285309 (2011).

[7]T. Tybell, P. Paruch, T. Giamarchi, and J.-M. Triscone, Phys. Rev. Lett. **89**, 097601 (2002).

[8]A. Agronin, M. Molotskii, Y. Rosenwaks, G. Rosenman, B. J. Rodriguez, A. I. Kingon, and A. Gruverman, J. Appl. Phys. **99**, 104102 (2006).

[9]P. Paruch, T. Giamarchi, T. Tybell, and J.-M. Triscone, J. Appl. Phys. **100**, 051608 (2006).

[10]S. V. Kalinin, A. N. Morozovska, L.-Q. Chen, and B. J. Rodriguez, Rep. Prog. Phys. **73**, 056502 (2010)

[11]A. Y. Emelyanov, Phys. Rev. B **71**, 132102 (2005).

[12]D. Li and D. A. Bonnell, Ann. Rev. Mater. Res. **38**, 351 (2008).

[13]A. N. Morozovska, E. A. Eliseev, Y. Li, S. V. Svechnikov, P. Maksymovych, V. Y. Shur, V. Gopalan, L.-Q. Chen, and S. V. Kalinin, Phys. Rev. B **80**, 214110 (2009).

[14]A. N. Morozovska, E. A. Eliseev, and S. V. Kalinin, Appl. Phys. Lett. **89**, 192901 (2006).

[15]R. C. Miller and A. Savage, Phys. Rev. **112**, 755 (1958).

[16]R. C. Miller and G. Weinreich, Phys. Rev. **117**, 1460 (1960).

[17]Y.-H. Shin, I. Grinberg, I.-W. Chen, and A. M. Rappe, Nature **449**, 881 (2007).

[18]W. J. Merz, Phys. Rev. **95**, 690 (1954).

[19]Nanoscale Characterisation of Ferroelectric Materials, edited by M. Alexe and A. Gruverman (Springer, Berlin/New York, 2004)

[20]T. Jungk, Á. Hoffmann, and E. Soergel, New J. Phys. **10**, 013019 (2008).

[21]D. Dahan, M. Molotskii, G. Rosenman, and Y. Rosenwaks, Appl. Phys. Lett. **89**, 152902 (2006).

[22]V. Bermúdez, L. Huang, D. Hui, S. Field, and E. Diéguez, Appl. Phys. A **70**, 591 (2000).

[23]Y. L. Chen, J. J. Xu, X. J. Chen, Y. F. Kong, and G. Y. Zhang, Opt. Commun. **188**, 359 (2001).

[24]L. H. Peng, Y. C. Fang, and Y. C. Lin, Appl. Phys. Lett. **74**, 2070 (1999).

[25]Y. Chen, C. Lou, J. Xu, S. Chen, Y. Kong, G. Zhang, and J. Wen, J. Appl. Phys. **94**, 3350 (2003).

[26]M. Maruyama, H. Nakajima, S. Kurimura, N. E. Yu, and K. Kitamura, Appl. Phys. Lett. **89**, 011101 (2006).

[27]K. Nakamura, J. Kurz, K. Parameswaran, and M. M. Fejer, J. Appl. Phys. **91**, 4528 (2002).

[28]Y. L. Chen, J. Guo, C. B. Lou, J. W. Yuan, W. L. Zhang, S. L. Chen, Z. H. Huang, and G. Y. Zhang, J. Cryst. Growth **263**, 427 (2004).